TURKISH ENERGY, NUCLEAR AND MINERAL RESEARCH AGENCY
TURKISH JOURNAL OF NUCLEAR SCIENCES
E-ISSN: 2791-7185
https://dergipark.org.tr/tr/pub/tjns

Reliability Computation of Kinetic Energy Based Shannon Entropy for Tritium Plasma Graphene Interactions

Alper Pahsa [1,*]

[1] **Havelsan Inc, Air C4ISR Systems, Ankara, 06510, Türkiye**

ARTICLE INFO

Article History:
Received April 20, 2025
Available online June 30, 2025

Research Article

Keywords:
Material Reliability of Graphene with Kinetic Energy
PMI of Tritium on Graphene
Tokamak reactor graphene material reliability
Tritium based fusion reactor material reliability
Fusion reactor kinetic energy based reliability

ABSTRACT

When selecting reactor building elements, it is important to consider the structural reliability of Tokamak fusion reactors. Fusion reactions generate substantial heat and energy, which can alter the structure of reactor walls, thereby diminishing the efficiency of energy production in reactors. The primary materials employed for walls in fusion reactors include tungsten, beryllium, and graphene, owing to their high melting points. This study looks at how tritium plasma ions, which have energies between 5 and 35 keV, affect graphene wall surfaces using molecular dynamics simulations, and also assesses the system's Kinetic Energy using Shannon entropy modeling. We use this information to compute the Weibull distribution's reliability prediction for graphene structures.

1. Introduction

The Population growth and rising living standards are increasing energy demand, a serious issue in this century. Most of the energy is originated from depleting fossils. Sustainability is the main feature that is required by the nuclear and renewable energy [1-2]. Energy is created at the final stage of exothermic nuclear processes; fission and fusion are crucial nuclear processes. An unstable, big nucleus is splitted into two or more smaller particles that releases energy at the output. Fission processes are the main source of power in todays current most nuclear reactors of today. Nuclear fusion process is made up of fusing the several nuclei. It produces nuclear and subatomic particles. Energy is created as the mass changes in reactants and products in the process. Nuclear fusion process requires 100 million degrees in its process. That is why the nuclear fusion is preferred in the researches of today and future studies in which has an unlimited fuel worldwide. Safe fusion reactors for instance, produces transient radioactive waste [3-6] in their processes. The most famous fusion reaction is the process that uses tritium and deuterium. The 14 MeV neutron from this event warms water to make turbine steam. Additionally, this reaction yields 3.5 MeV He [7-9]. The produced Helium of the fusion product reactor is the input nuclei of the Deuterium and Tritium under a huge amount of heated plasma [10-11]. Classic thermonuclear fusion reactors use magnetic fields to densify the plasma. Magnetic fields trap plasma from the reactor's first wall. High-energy plasma influences barriers. The divertor zone has the highest attrition because magnetic field lines convey lower-energy plasma to the wall. Plasma-first wall materials and interactions are studied in fusion. Plasma must yield fusion helium. Helium interacts with divertor walls during removal [12-13]. Dying divertor and reactor walls discharge neutrons. Tungsten, beryllium, molybdenum, steel, and graphene inhibit tokamak reactor wall erosion. High melting point and atomic number make tungsten plasma-resistant [11-13]. Nuclear fusion reactor structural reliability analysis is unusual in reliability literature. General studies are performed for nuclear fission reactors as in structural reliability analysis. For instance [14] examines nuclear fission power plant structural system and component structural analysis with probabilistic analysis methods in determining the longevity, dependability, and danger. This source uses probability, material science, fluid, fracture, and structural mechanics. Most nuclear fusion reactors' main issue is fusion reactions. Literature understates structure reliability. In [15], recent structural and thermomechanical research are discussed including the magnet, diagnostic, and reproductive coverage. Safe and dependable systems affect fusion device dependability for creating the trust. Wendelstein 7-X, DEMO, and ITER fusion equipment for energy generation or experiments are assessed for availability, maintainability, and inspectability [13]. This study includes solely fusion device basics. Commercial plasma applications with surface coating are best for

*Corresponding author: apahsa@havelsan.com.tr

Tokamak fusion reactor structure reliability testing. Space-based plasma-facing structures must resist radiation and particles. Plasma-facing structures must resist radiation and particles to limit space impacts [15-19]. Tokamak nuclear fusion reactor walls struggled to maintain tritium. Plasma-facing graphene magnetic fusion loses tritium. Plasma tritium retention was 40% and 51% for JET and TFTR. After experiments, fusion reactor sanitization took 12–16%. Walls of titanium. To Recent calculations predict that the French experimental Tokamak reactor ITER will approach its tritium limit after 100 pulses. Rising tritium levels stretch reactor walls, shortening life. This affects thermal-to-electric energy transfer in fusion. This study used molecular dynamics simulations to develop a graphene wall structure with bigger crystal atomic patterns. In thermonuclear reactors like ITER and DEMO, where harsh conditions (high temperatures, intense neutron radiation) make traditional detectors difficult to use, graphene is being investigated as a potential material for magnetic field sensors and structural elements. Research shows that graphene-based Hall effect sensors, especially those made on silicon carbide (SiC) substrates, are remarkably resistant to radiation and retain their high sensitivity even when exposed to rapid doses of neutrons. The MARIA reactor's research verified that although neutron irradiation changes the density of charge carriers, the majority of damage is inflicted on the hydrogen passivation layer instead of the graphene, indicating the possibility of self-healing at elevated temperatures. Apart from sensors, graphene-reinforced metal nanocomposites (such those with Cu, Ni, or V) show enhanced radiation endurance by trapping flaws at interfaces, making them promising choices for reactor walls and structural materials. Moreover, graphene and carbon nanotubes are recommended for first-wall applications due to their low neutron absorption, thermal stability, and possibility for integrated cooling through capillary fluid transfer. However, molecular dynamics study emphasizes the need for perfect fabrication by showing how composite performance might be hampered by pre-existing graphene damage. Graphene's unique properties make it a crucial component for the development of fusion technology, despite persistent challenges with substrate optimization and hydrogen layer replacement.

Graphene coatings may have a number of benefits over more conventional materials like tungsten or carbon composites, according to recent research on the retention of tritium in graphene-based tokamak wall designs. According to research, few-layer graphene's poor hydrogen isotope solubility and rapid diffusion rates, which promote tritium desorption, can lower tritium retention by up to 70% when compared to graphite (e.g., Zhang et al., 2024 in Nuclear Fusion). Furthermore, the damage caused by plasma exposure is lessened by graphene's better heat conductivity and radiation resistance. However, issues remain with adhesion stability at high heat fluxes and potential defect-induced trapping at grain boundaries (Lee et al., 2023, Applied Surface Science). While graphene-covered test tiles on EAST and DIII-D show promising reductions in co-deposition, the effects of prolonged exposure to neutrons are still being investigated. Graphene's scalability may enable self-cleaning walls with smaller tritium reserves, but more research is required before big divertors can employ it.

The following figure 1 shows the initial configuration of the study model system in the simulation:

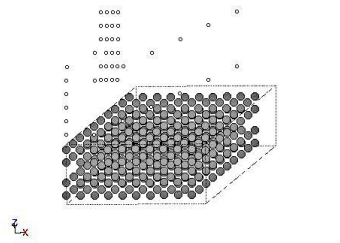

Figure 1. Initial configuration top surface of the molecular dynamics simulation model

In the study the reliability function of the two-parameter Weibull distribution to assess the material's reliability. This information is used by the 2-parameter Weibull distribution's reliability function to evaluate the material's dependability. A major objective of the literature is to investigate the fusion plasma material interactions in the wall constructions of Tokamak fusion reactors. In temperature-changing chambers, plasma-material interactions take place similarly to how tritium plasma modifies the surface of the reactor inner chamber materials. For example, lifecycle reliability estimates and design are needed for graphene on the walls of the Tokamak nuclear fusion reactor when tritium retentions are present. The only studies in the literature that address tritium plasma retention, tritium redepositing, and the boronization effects of the tritium in fusion reactor studies are Tritium Retention Breeding and Tritium Retention in the Gaps of Tungsten Wall Structures of the JET, MAST, EAST, and ITER DEMO experimental fusion reactors. Being the first structural reliability investigation on the retention of tritium on the material structures of graphene reactor walls, this work closes a gap in the literature.

2. Materials and Methods

2.1. Materials

Molecular dynamics simulations were conducted utilizing the Python programming language. Version 6.0.3 of Spyder, part of the Anaconda module, was utilized to complete this task. Calculations were performed on a Dell Precision 7680 equipped with an Intel Core i7 13th Generation processor, operating on Ubuntu 24.10 Linux. The version of the Python compiler utilized was 3.12.7. This study utilizes

the Atomic Simulation Environment (ASE [20]), a Python framework designed for molecular dynamics simulations in figure 2:

Figure 2. Atomic Simulation Environment in Python language for Molecular Dynamics Simulation

2.2. Methods

The retention mechanism was developed through the simulation of a significant amount of graphite, comprising approximately 1,200 carbon atoms. The findings demonstrated that retention efficacy was influenced by multiple factors, such as the pressure and temperature conditions present during the simulation. The findings have important implications for future research on carbon-based materials and their diverse applications across various sectors. Graphene is treated as the C hexagonal crystal structure. For the sake of simplicity size of the simulated material molecular calculations tritium is treated with the single hydrogen atoms. In the molecular dynamics Carbon atoms in Figure 2 symbolized in gray color and the tritium (hydrogen) atoms in Figure 2 are given as white color. The block underwent exposure to hydrogen at energy levels between 5 and 35 keV with 3T magnetic induction force to enable calculations and substitute tritium. The selected energy levels for the simulation were adequate, as demonstrated by the current simulations covering a suitable range of collision energy, as reported in the literature. Initialization of the molecular dynamics algorithm parameters are stated below:

Parameters

a1 = 2.46 # Lattice constant for graphene (in Angstrom)

c1 = 6.70 # Interlayer spacing for graphene (in Angstrom)

num_hydrogen_atoms = 42

timestep = 1.0 # fs

total_steps = 200

temperature = 300 # K

vacuum=True

orthogonal=True

periodic=True

bulk_cutoff = 5.0 # Distance cutoff for retention (Angstroms)

h = 3 #distance between tritium and graphen surface

energy_H = 5 to 35 # keV initial energies

magnetic_field = 3.0 # Magnetic field in Tesla

hydrogen_mass = 1.00784 * 1.66053906660e-27 * units.kg # Mass of hydrogen atom

hydrogen_charge = 1 * units.C # Charge of hydrogen ion (H+)

In this study, the potential for the simulation configurations of the materials are used is the Effective Medium Theory (EMT) potential defined in the ASE python framework. EMT is developed from averaging the multiple values of the constituents that directly make up the composite materials that are in electromagnetic environment. Effective permittivity of the materials as a whole is calculated in the acceptable approximations.

Thermal equilibrations were performed with residual graphene under controlled conditions at a temperature of 300K. A significant number of these were conducted. For one second, the surface layers were free to move due to the magnetic force hits applied by the microcanonical (NVE) ensemble. This made it easy for these layers to move. This is made possible by the mechanism that keeps the ensemble's energy, volume, and elements constant. The upper four layers were Langevin-thermostatized for one picosecond after the NVE cycle to disperse the heat generated by the bombardment.The integral of Newton's Second Law of Motion is employed to simulate the motion of a group of particles (atoms or molecules) in molecular dynamics, a calculation model. The i-th atom's motion is denoted as [21]:

$$m_i x_i = -\nabla U_i \tag{1}$$

in (1) m_i is the mass, x_i is the position and U_i is an interatomic potential energy function that describes the interaction between each atom and its neighbors. The molecular dynamics simulation of the hcp function of ASE generates a graphene structure within a substantial graphite crystal. The hydrogen atoms are randomly dispersed within the graphite lattice, with a starting kinetic energy ranging from 5 keV to 35 keV with an electromagnetic force of 3T. In molecular dynamics simulations, the Velocity-Verlet approach is employed to simulate the system's dynamics [22-24]. Then in the simulation kinetic energy based Shannon Entropy is computed to the system simulation model configuration. Utilizing the atom positions corresponding kinetic energies, we compute the Shannon entropy of the system in this simulation. According to Shannon, the set of probabilities can be identified as p1, p2, p3,..., pn, which results in vagueness through (H) measurement. The Shannon entropy is provided as [25-26] when the atoms' positions in this system model are implemented:

$$H = K \sum_{i=1}^{n} p_i log_2 p_i \tag{2}$$

The Shannon entropy and associated probabilities p1, p2, p3,..., pn are displayed in Equation (2). These probabilities relate to the atomic model used to set up the system in molecular dynamics and the frequency of atom appearance. The calculation of the Shannon Entropy is performed by using the kinetic energy values of the corresponding atom positions. Each kinetic energy information is selected with the bins of 50 and based on the sampled bins the histogram is calculated. Based on the histogram and the summation of the histogram probabillity is derived and by using (2) formulation Shannon Entropy based on the kinetic energy values are calculated. The Weibull reliability distribution is defined by the calculated kinetic energy based Shannon entropy values. Based on the above procedure, Kinetic Energy based Shannon Entropy is then used to calculate the material reliability calculation based on Weibull distribution. The three-parameter Weibull distribution equation is as follows [27-28].

$$R(t) = e^{-(\frac{t-\gamma}{\alpha})^{\beta}} \quad (3)$$

where t denotes the irradiation duration (), γ is the location parameter, β is the shape parameter (slope) (β>0), and α is the scale parameter (characteristic life) (α>0). In computations, it is a widely held belief that γ=0, as it denotes the displacement of the origin in the dependability distribution graph. The probability-of-failure function is defined as follows:

$$F(t) = 1 - R(t) \quad (4)$$

$$1 - F(t) = e^{-(\frac{t}{\alpha})^{\beta}} \quad (5)$$

In the previously mentioned context, γ equals zero, and the specified conditions for F(t) are 0 < F(t) < 1. In order to satisfy the mandated criteria, the equation is adjusted.

$$ln(ln\frac{1}{1-F(t)}) = \beta lnt - \beta ln\alpha \quad (6)$$

The following is generated when the equation is created in the configuration of y=mx+n:

$$y(t) = ln(ln\frac{1}{1-F(t)}), \; m=\beta \text{ and } n=-\beta ln\alpha \quad (7)$$

Bernard Approximation for Median Ranks is utilized to calculate the unreliability parameters for each failure [31]. Then the unreliability parameter became:

$$F(t) = MedianRank = \frac{Rank-0,3}{N+0,4} \quad (8)$$

where N is the dataset's maximum number of orders, and rank is the order number in the tables given in the results section.

3. Results and Discussion

The simulation bombards the graphene crystal with hydrogen ions at energies ranging from 5 keV to 35 keV, utilizing a magnetic field strength of 3T. The next phase of the procedure entails the execution of molecular dynamics simulations. Graphene construction comprises multiple layers to facilitate the integration of thermostats. This sequence demonstrates the Shannon Entropy based on the kinetic energy calculations of the molecular configuration, as well as the three-dimensional molecular dynamics simulation results. The duration of the simulation process, the retention count from the molecular simulation model, the rank, the F(t) function, the natural logarithm of the kinetic energy based Shannon Entropy, the y(t) function linked to the kinetic energy Shannon Entropy, and the reliability based on the y(t) function for tritium affected by kinetic energies between 5 keV and 35 keV with a 3T magnetic induction force are all shown in Tables 1, 2, 3, and 4.

Table 1. Kinetic energy based Shannon Entropy F(t) and y(t) values calculated by equations 3, 4, 5, 6 and 7 for Tritium with 5keV bombardment with 3T on Graphene Crystal

Process Time (fs)	Kinetic Energy Shannon Entropy of the total bulk surface	Rank	F(t)	Ln (Shannon Kinetic Eng)	y(t)_ Shannon Kinetic Eng
0	-4	1	0,074468085	0	1
25	4	2	0,180851064	1,386294361	0,206529857
50	5,8	3	0,287234043	1,757857918	0,176563403
75	6	4	0,393617021	1,791759469	0,159948474
100	5,75	5	0,5	1,749199855	0,148611365
125	5,65	6	0,606382979	1,731655545	0,140090081
150	5,7	7	0,712765957	1,740466175	0,133310901
175	5,9	8	0,819148936	1,774952351	0,127711149
200	5,95	9	0,925531915	1,78339122	0,122960135

Table 2. Kinetic energy based Shannon Entropy F(t) and y(t) values calculated by equations 3, 4, 5, 6 and 7 for Tritium with 15keV bombardment with 3T on Graphene Crystal

Process Time (fs)	Kinetic Energy Shannon Entropy of the total bulk surface	Rank	F(t)	Ln (Shannon Kinetic Eng)	y(t)_ Shannon Kinetic Eng
0	-4	1	0,074468085	0	1
25	4,95	2	0,180851064	1,599387577	0,198968365
50	5,8	3	0,287234043	1,757857918	0,168116675
75	5,98	4	0,393617021	1,788420568	0,151118198
100	6,1	5	0,5	1,808288771	0,139573118
125	6,3	6	0,606382979	1,840549633	0,130928245
150	6,5	7	0,712765957	1,871802177	0,124072886
175	6,45	8	0,819148936	1,864080131	0,118426234
200	6,55	9	0,925531915	1,87946505	0,11364758

The latest column in the table 1,2,3,4 determines the reliability values based on kinetic energy based Shannon Entropy. For the latest column the reliability characteristic graphs for the system is drawn for comparing it to the Weibull hazard probability distribution graph. Figures 3, 4, 5, and 6 present the kinetic energy-based Shannon entropy and the corresponding graphs, respectively:

Upon observing Figures 3, 4, 5, and 6, both graphs exhibit a resemblance to the Weibull distribution probability density function associated with the hazard function. In which the R2 values of graphical fit test

Table 3. Kinetic energy based Shannon Entropy F(t) and y(t) values calculated by equations 3, 4, 5, 6 and 7 for Tritium with 25keV bombardment with 3T on Graphene Crystal

Process Time (fs)	Kinetic Energy Shannon Entropy of the total bulk surface	Rank	F(t)	Ln (Shannon Kinetic Eng)	y(t)_ Shannon Kinetic Eng
0	-4	1	0,074468085	0	1
25	3,75	2	0,180851064	1,32175584	0,18345641
50	5	3	0,287234043	1,609437912	0,150723429
75	5,85	4	0,393617021	1,766441661	0,132965227
100	5,9	5	0,5	1,774952351	0,121042209
125	5,95	6	0,606382979	1,78339122	0,112197999
150	5,85	7	0,712765957	1,766441661	0,105240905
175	6,2	8	0,819148936	1,824549292	0,099551042
200	6,25	9	0,925531915	1,832581464	0,094766473

Table 4. Kinetic energy based Shannon Entropy F(t) and y(t) values calculated by equations 3, 4, 5, 6 and 7 for Tritium with 35keV bombardment with 3T on Graphene Crystal

Process Time (fs)	Kinetic Energy Shannon Entropy of the total bulk surface	Rank	F(t)	Ln (Shannon Kinetic Eng)	y(t)_ Shannon Kinetic Eng
0	-4	1	0,074468085	0	1
25	3,85	2	0,180851064	1,348073148	0,205324751
50	5,75	3	0,287234043	1,749199855	0,175198344
75	6	4	0,393617021	1,791759469	0,158511436
100	5,95	5	0,5	1,78339122	0,147133639
125	5,9	6	0,606382979	1,774952351	0,138586928
150	5,8	7	0,712765957	1,757857918	0,131791019
175	5,75	8	0,819148936	1,749199855	0,126179989
200	5,85	9	0,925531915	1,766441661	0,121421338

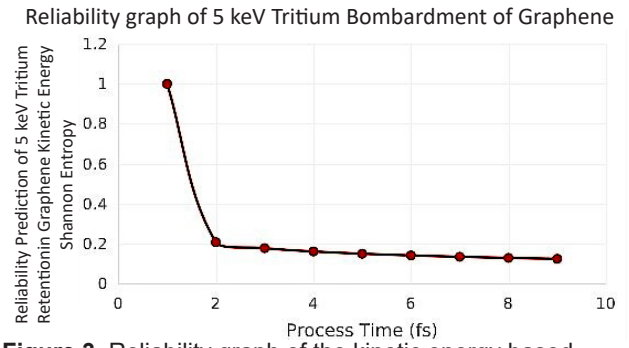

Figure 3. Reliability graph of the kinetic energy based Shannon Entropy of the simulated system at 5keV bombardment of Tritium with 3T magnetic induction force

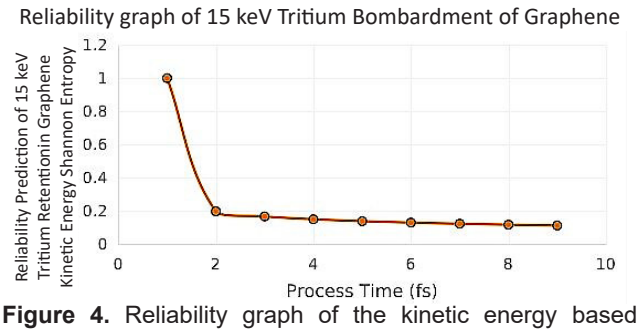

Figure 4. Reliability graph of the kinetic energy based Shannon Entropy of the simulated system at 15keV bombardment of Tritium with 3T magnetic induction force

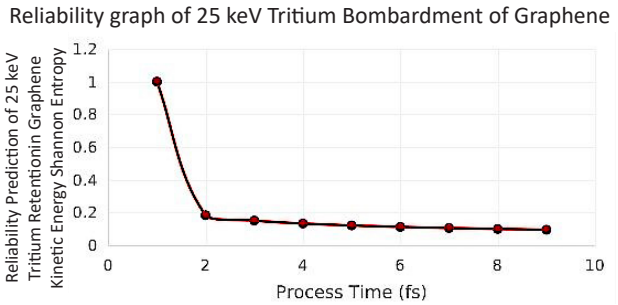

Figure 5. Reliability graph of the kinetic energy based Shannon Entropy of the simulated system at 25keV bombardment of Tritium with 3T magnetic induction force

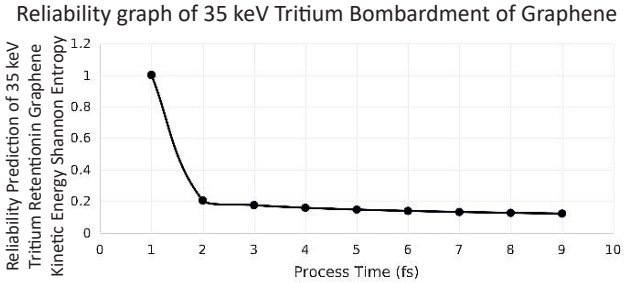

Figure 6. Reliability graph of the kinetic energy based Shannon Entropy of the simulated system at 35keV bombardment of Tritium with 3T magnetic induction force

results are calculated and the graphical fit given for the Weibull probability fit test plots are given in the following figures 7, 8, 9, and 10.

The Figure 7 shows the transformed data points against the theoretical quantiles of Weibull distribution for 5 keV tritium plasma process of Shannon Entropy calculated based on kienitc energy. The points roughly follow the red regression line, with the R2=0.8718 which shows that the Weibull distribution is a good fit for Shannon Entropy based on kinetic energy at 5 keV energy of tritium plasma.

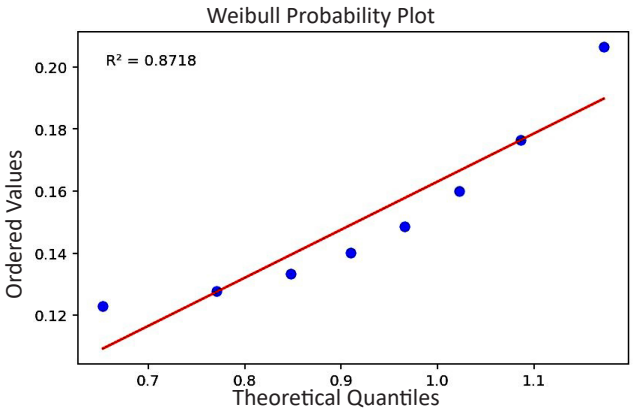

Figure 7. Graphical Fit Test Weibull Probability Plot for 5keV based tritium Shannon Entropy calculated based on kinetic energy

The Figure 8 shows the transformed data points against the theoretical quantiles of Weibull distribution for 15 keV tritium plasma process of Shannon Entropy calculated based on kienitc energy. The points roughly follow the red regression line, with the R2=0.8395

which shows that the Weibull distribution is a good fit for Shannon Entropy based on kinetic energy at 15 keV energy of tritium plasma.

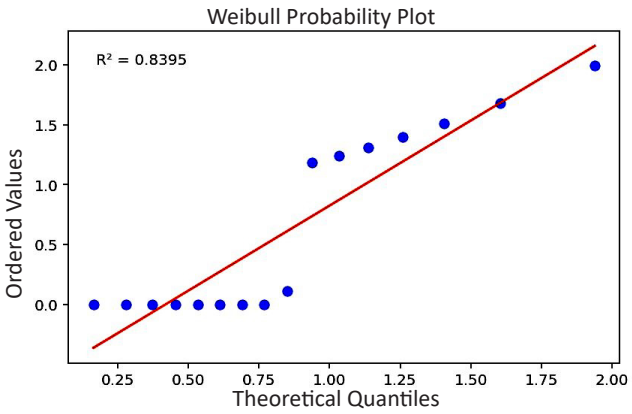

Figure 8. Graphical Fit Test Weibull Probability Plot for 15keV based tritium Shannon Entropy calculated based on kinetic energy

The Figure 9 shows the transformed data points against the theoretical quantiles of Weibull distribution for 25 keV tritium plasma process of Shannon Entropy calculated based on kienitc energy. The points roughly follow the red regression line, with the R2=0.8105 which shows that the Weibull distribution is a good fit for Shannon Entropy based on kinetic energy at 25 keV energy of tritium plasma.

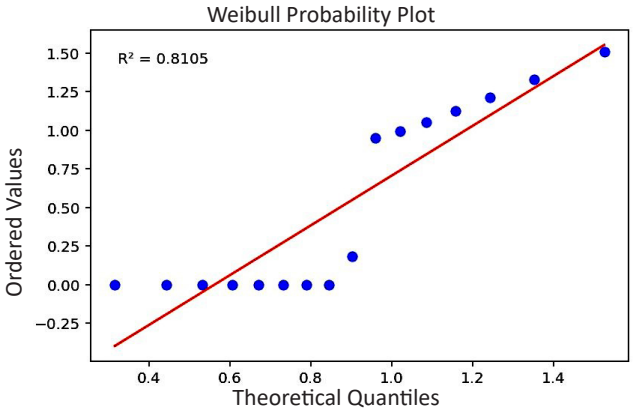

Figure 9. Graphical Fit Test Weibull Probability Plot for 25keV based tritium Shannon Entropy calculated based on kinetic energy

The Figure 10 shows the transformed data points against the theoretical quantiles of Weibull distribution for 35 keV tritium plasma process of Shannon Entropy calculated based on kienitc energy. The points roughly follow the red regression line, with the R2=0.7797 which shows that the Weibull distribution is a good fit for Shannon Entropy based on kinetic energy at 35 keV energy of tritium plasma. As the applied kinetic energy of tritium plasma is increased from 5keV to 35keV the calculated Shannon Entropy based on the molecular dynamics system calculated kinetic energy the Entropy of irregularities are increased. For instance all of the calculated 5keV, 15keV, 25keV and 35keV corresponding Shannon Entropies based on system kinetic energy calculated Weibull distribution reflect the same approximate values. It is obvious the system is unreliable and show the effect of the retention because of the tritium atoms are bounded to the graphene “C” atoms to hold them in the crystal structure.

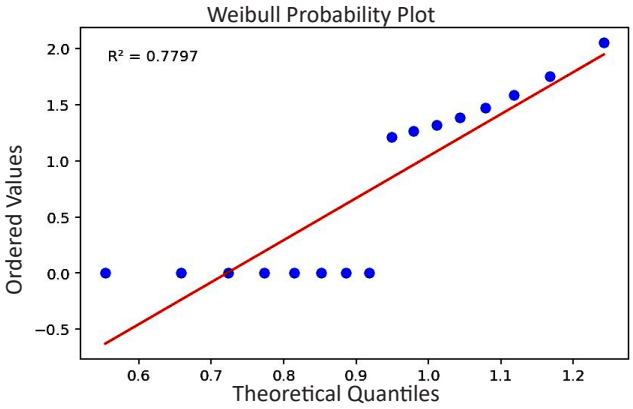

Figure 10. Graphical Fit Test Weibull Probability Plot for 35keV based tritium Shannon Entropy calculated based on kinetic energy

4. Conclusions

The material choices required for plasma-based energy devices, such as fusion Tokamak reactors and space propulsion systems, are assessed by the graphs presented in the previous results. The estimated results indicate that the Weibull distribution, which incorporates Shannon entropy calculations based on the system kinetic energy, is a valuable method for evaluating the reliability of structures when they interact with plasma and materials. From the given results above the Shannon Entropy based on the kinetic energy of the system can be used as a feature in determining the reliability prediction of the structure materials. Since this study is based on molecular dynamics simulations for tritium plasma interaction with the graphene, the experimental tokamak reactor fusion with graphene wall materials during the operational effects of tritium plasma as a fuel in fusion process is necessary to perform for future studies. In the computation of the structural reliability of events that entail contact with plasma material, the Weibull distribution is advantageous. This study complemented the objective of Shannon Entropy based on the system kinetic energy parameter based Weibull distribution prediction can be used in the reliability calculation of the fusion reactor wall structures. So that the nuclear fusion reactor wall material selection and design criteria can use the Weibull reliabilities calculated parameters as a requirement by the designers of the tokamak type fusion reactors. Likewise the nuclear fission sector use the structural reliability in pumps and pipes, nuclear fusion Tokamak type of reactors will utilize this technique with the same perspective in the structural components of vacuum vessel, In-vessel, test blanket modules and diagnostics. The Weibull method can be employed to examine plasma material interactions

in forthcoming studies of plasma parameters. Future investigations on plasma collisionality and anode/cathode sputtering are viable. The operational efficacy, safety, and security of Tokamak fusion reactors are ensured by their structural integrity. This includes the selection of appropriate materials, the assessment of wear and damage via surface roughness measurements, the management of heat and stress during plasma operations, the application of Weibull analysis to gauge reliability, and the implementation of regular maintenance.

Author Contribution Statement

The study's conception and design were the collaborative efforts of all authors. The authors themselves conducted the material preparation, data collection, and analysis.

References

[1] Ongena J., “Nuclear fusion and its large potential for the future world energy supply”, 2016, Nukleonika Journal, pp:425-432, web site ref: https://sciendo.com/pdf/10.1515/nuka-2016-0070

[2] Takeda S., Pearson R.Nuclear Fusion Power Plants. Power Plants in the Industry. 2018; Chap 6: 101-122, IntechOpen publishing, website ref: https://www.intechopen.com/chapters/62970, DOI: 10.5772/intechopen.80241

[3] IAEA.Fusion Energy for Peace and Sustainable Development. IAEA. Vienna. 2018: 2-18. web site ref: https://nucleus.iaea.org/sites/fusionportal/SiteAssets/18-03925E_BRO_Fusion.pdf

[4] IAEA.Kikuchi M., Lackner K., Tran M. Q.Fusion Physics. Vienna. 2012: 20-21, web site ref: https://wwwpub.iaea.org/MTCD/Publications/PDF/Pub1562_web.pdf

[5] Ibrahim S., Lahboub F. Z., Brault P., Petit A., Caillard A., Millon E., Sauvage T., Fernandez A., Thomann A.L.Influence of helium incorporation on growth process and properties of aluminum thin films deposited by DC Magnetron sputtering.Surface and Coatings Technology.2021; Vol;426, web site ref: https://www.sciencedirect.com/science/article/abs/pii/S0257897221009828, https://doi.org/10.1016/j.surfcoat.2021.127808

[6] Behrish R., Harries D. R.International Atomic Energy Agency.Lifetime Predictions For The First Wall and Blanket Structure of Fusion Reactors.Proceedings of a Technical Committee Meeting.Karlsruhe. Nuclear Fusion J. 1986; Vol: 26, DOI 10.1088/0029-5515/26/5/015

[7] IoP Publishing Ltd. Nuclear Fusion Half a Century of Magnetic Confinement Fusion Research.2002:230-258, web site ref: https://library.psfc.mit.edu/catalog/online_pubs/conference%20proceedings/fusion%20energy%20conferences/Nuclear%20Fusion%20(IOP)%20half%20a%20century.pdf

[8] Kotov V.Particle conservation in numerical models of the tokamak plasma edge. Physics Plasma Ph Archive. Forschungszentrum Jülich GmbH, Institut für Energie- und Klimaforschung-Plasmaphysic.Partner of the Trilateral Euregio Cluster.Jülich, Germany, 2017; Vol 24, https://doi.org/10.1063/1.4980858

[9] K. Wojcyzkowski. New Development in Corrosion Testing: Theory, Methods and Standards.AESF Foundation, Plating and Surface Finishing.2011; Vol January, web site ref: https://www.pfonline.com/articles/new-developments-in-corrosion-testing-theory-methods-andstandards

[10] Linden T.Compact Fusion Reactors.CERN Colloquium. Helsinki Institute of Physics 2015; Vol March, web site ref: http://cds.cern.ch/record/2004827

[11] L. Rajablou, S.M. Motevalli, F. Fadaei.Study of alpha particle concentration effects as the ash of deuterium-tritium fusion reaction on ignition criteria.Physica Scripta.2022; Vol 97, No 9: DOI 10.1088/1402-4896/ac831a

[12] Malo M., Morono A., Hodgson E. R.Plasma Etching to Enhance the Surface Insulating Stability of Aluminumina for Fusion Applications.Nuclear Materials and Energy. Elsevier.2016; Vol 9: 247-250, DOI:10.1016/j.nme.2016.05.008

[13] Miyamoto K.Fundamentals of Plasma Physics and Controlled Fusion.2011.3rd Edition: 1-21, web site ref: https://www.nifs.ac.jp/report/NIFS-PROC-88.pdf, DOI 10.1088/0029-5515/38/4/701

[14] Cronvall O., “Structural lifetime, reliability and risk analysis approaches for power plant components

and systems”, Espoo 2011, pp. 69, VTT Publications 775.

[15] Arena P., Maio P. A.Special Issue .Structural and Thermo-Mechanical Analysis in Nuclear Fusion Reactors.MDPI Applied Sciences.2020;web site ref: https://www.mdpi.com/journal/applsci/special_issues/Fusion_Reactors, https://doi.org/10.3390/app122412562

[16] Apostolakis G. E., Sanzo D. L. Limiter Probabilistic Lifetime Analysis. Fusion Engineering and Design. 1988;Vol. 6:229-267, https://doi.org/10.1016/S0920-3796(88)80111-X

[17] Du, X.Unified Uncertainty Analysis by the First Order Reliability Method.J. Mech. Des. 2008; Vol 30 (9): 091401-09410, DOI:10.1115/1.2943295

[18] Freidberg J.P., Mangiarotti F.J., Minervini J. Desgining a Tokamak Fusion Reactor-How Does Plasma Physics Fit In?. Plasma Science and Fusion Center.Massachusetts Insitute of Technology, Cambridge MA.2015; Vol June; 16.,https://doi.org/10.1063/1.4923266

[19] Fusion Energy Sciences Workshop.On Plasma Material Interactions-Report on Science Challanges and Research Opportunities in Plasma Material Interactions. U.S. Department of Energy, Office of Science, France, Fusion Energy Sciences, 2015

[20] Ask Hjorth Larsen, Jens Jørgen Mortensen, Jakob Blomqvist, Ivano E. Castelli, Rune Christensen, Marcin Dułak, Jesper Friis, Michael N. Groves, Bjørk Hammer, Cory Hargus, Eric D. Hermes, Paul C. Jennings, Peter Bjerre Jensen, James Kermode, John R. Kitchin, Esben Leonhard Kolsbjerg, Joseph Kubal, Kristen Kaasbjerg, Steen Lysgaard, Jón Bergmann Maronsson, Tristan Maxson, Thomas Olsen, Lars Pastewka, Andrew

Peterson, Carsten Rostgaard, Jakob Schiøtz, Ole Schütt, Mikkel Strange, Kristian S. Thygesen, Tejs Vegge, Lasse Vilhelmsen, Michael Walter, Zhenhua Zeng, Karsten Wedel Jacobsen, “The Atomic Simulation Environment—A Python library for working with atoms”, Phys.: Condens. Matter Vol. 29 273002, 2017

[21] Gonzalez A. M., “Force Fields and Molecular Dynamics Simulations”, pp: 169-200, EDP Sciences, 2011

[22] Bedoya F., “Plasma facing components conditioning techniques and their correlation with plasma performance in the national spherical Torus experiment upgrade (NSTX-U)”, [Doctoral Dissertation]. Urbana-Champaign, IL: University of Illinois at Urbana-Champaign, Illinois Digital Environment for Access to Learning and Scholarship 2017. Available at: http://hdl.handle.net/2142/99444

[23] Schneider T, Stoll E., “Molecular-dynamics study of a three-dimensional one-component model for distortive phase transitions.”, Phys Rev B (1978) 17:1302–22.

[24] Timonova M, Thijsse BJ., “Molecular Dynamics simulations of the formation and crystallization of amorphous Si”, Comput Mater Sci, 50(8):2380–90, 2011.

[25] K. Wojcyzkowski.New Development in Corrosion Testing: Theory, Methods and Standards.AESF Foundation, Plating and Surface Finishing.2011; Vol January, web site ref: https://www.pfonline.com/articles/new-developments-in-corrosion-testing-theory-methods-andstandards

[26] Karaca Y, Moonis M., “Multi-Chaos, Fractal and Multi-Fractional Artificial Intelligence of Different Complex Systems”, Chapter 14, pp:231-245, Academic Press, 2022

[27] Kotov V.Particle conservation in numerical models of the tokamak plasma edge. Physics Plasma Ph Archive. Forschungszentrum Jülich GmbH, Institut für Energie- und Klimaforschung-Plasmaphysic.Partner of the Trilateral Euregio Cluster.Jülich, Germany, 2017; Vol 24, https://doi.org/10.1063/1.4980858

[28] Asadi S. Panahi H., Anwar S., Lone S. A.Reiability Estimation of Burr Type III Distribution under Improved Adavtive Progressive Censoring with Application to Surface Coating.Eksploatacja i Niezawodnosc-Maintenance and Reliability.2023;Vol 25, Issue 2, https://doi.org/10.17531/ein/163054